

# Study of the Operating Cost of the Electric Pump for Mine Dewatering: Case of the SOMAÏR Uranium Mine

## Abstract

This study focuses on the operating cost of the electric pump used to extract water from the Artois mine owned by Société des Mines de l'ÀÏR. Exploitation of the SOMAÏR Artois mine uranium deposit is to be increased from the 20 m level to the 80, 100 or 120 m level; in the current phase of certain pits, access to the uranium deposit can only be achieved by a means that can draw off the water encountered. It is therefore essential to set up a drainage system to manage and evacuate the various water inflows. The main source of incoming water is the nearby water table, which is drained directly onto the mining unit. The current drainage system has two sumps capable of storing the various water inflows without incident. The energy balance for the three (3) years of pumping was drawn up using the electricity consumption data received. Peaks appear in August for the year 2021, followed by January 2020 and May 2022. The results show that specific energy is high, resulting in higher power consumption than water production. According to the graph of performance curves  $P = f(Q)$ , the power ratings obtained for flows corresponding to the 24 m head are 25 kW at a flow rate  $Q = 49$  l/s for pump 261; 35 kW, at a flow rate  $Q = 59$  l/s for pump 259 and 35 kW at a flow rate  $Q = 105$  l/s for pump 234.

## Introduction

The successful exploitation of mineral resources requires that the mining project and subsequent mining operations be adapted to the natural conditions identified during the deposit documentation phase. One of the factors analyzed includes water conditions (hydrogeological and hydrological), which, in view of growing environmental awareness, are among the most important, both during the process of obtaining a mining permit and at the mining stage [1]. Groundwater influx into an underground mine will seriously affect its mine plan and the geological safety of the engineering[2]. In most cases, dewatering of open-pit mine workings is necessary to ensure the safety of preparatory work and mining operations. If a section to be mined becomes waterlogged, a drainage system is built, which drains the rock mass down to the depth of the bottom of the planned mining level [3]. In mines, water ingress during mining is one of the most difficult problems to control, and can even lead to the cessation of mining operations. This is why permanent dewatering before and during mining is essential, taking into account the site's hydrogeology and hydrology. This dewatering operation in mines consumes a great deal of energy, at a significant financial cost. In countries like India, for example, pumps account for around 18% of total energy consumption and contribute around 40% of the total electrical energy consumption of a typical open-pit mine [4][5].

Numerous studies have been carried out on the energy costs of pumps used for mine dewatering. In South Africa, [6] conducted a study on optimizing energy recovery in mine dewatering systems. According to the results of their work, a load of 1.5 MW could be shifted from Eskom's evening peak and 2.5 MW from the morning peak. For this case study, the potential savings in energy costs in the dehydration system resulting from these initiatives were R1.7 million per year. The new strategy proved effective when all equipment was available, and presented itself as a practical solution for reducing energy costs in mine dewatering systems. [7] investigated the energy-saving potential of open-pit mine drainage as part of his doctoral thesis. According to the results of his work for the mine studied, the results of the pumping methodology indicated that substantial energy savings could be achieved. The operations studied can displace 1,496,805 kWh out of the peak usage period, which translates into R2,107,609 in energy savings per year. Based on this case study, there is definite potential for savings in other open-pit mining operations in South Africa. [8] conducted a study to investigate the effects of automated control on mine dewatering pumps. The benefits of pump automation include electricity cost savings through load shifting, as well as preventive maintenance and pump protection procedures. Project performance was tested in manual control, programmed manual control, programmed surface manual control and automatic control. In the case study, manual intervention delivered the highest electricity cost savings. To achieve this saving, the system was depleted to such an extent that the columns and infrastructure began to fail. Automotive intervention delivered lower electricity cost savings, but proved more sustainable. Automatic intervention resulted in lower electricity savings than manual intervention. However, taking into account factors

such as infrastructure damage after a period of manual control, automatic intervention proved to be the best balance for controlling the mine's dewatering pumps, to achieve electricity savings and system sustainability.

Mining of the uranium deposit at SOMAÏR's Artois mine is set to increase from the 20 m level to the 80, 100 or 120 m level; in the current phase of certain pits, access to the uranium deposit can only be achieved by a means that can draw off the water encountered. It is therefore essential to set up a drainage system to manage and evacuate the various water inflows. According to the information received, the main source of water inflow is the nearby water table, which gushes out directly onto the mining unit. The current drainage system has two sumps capable of storing the various water inflows without incident.

The first is a pumping installation consisting of a raft-mounted high-pressure pump, while the second is a submerged low-pressure pump. The position of a sump or "albraque" varies according to the operation. An albraque is dug after careful studies showing the direction of water flow. High-pressure raft pumps (Flygt) have a discharge diameter of 100 mm, often reduced to 80 mm. Low-pressure (Flygt) submersible pumps are Ø80 mm, and a surface-mounted pump with a Ø200 mm load suction and Ø100 mm discharge replaces super-high-pressure submersible pumps. We use both flexible and rigid steel pipes.

The transition from the 20 m, 40 m and 80 m levels to the 120 m level by successive 20 m steps at SOMAÏR's Artois mine requires the design of a drainage system capable of coping with the various water inflows. For this reason, they need to be identified and quantified on the basis of parameters linked to the site's geology. The dewatering system consists of sumps or "albraques" which collect the water drained from the mine section, and whose capacity is determined on site by the hydrogeology section. A pumping installation with selected discharge and suction pipes is then set up to drain this water away from the mine field.

The aim of this study is therefore to evaluate the operating cost of the electric pump in the mine drainage at the Artois mine.

## **Materials and Methods**

### **Presentation of the Study Area**

SOMAÏR (Figure 1.) is located around 1,250 km from Niamey and 250 km northwest of Agadez (as the crow flies). Its creation in 1968 gave rise to the mining town of Arlit. Arlit is located in the heart of West Africa, around 2,000 km from the Atlantic Ocean and the Mediterranean, at coordinates 18° 48' latitude North and 07° 19' longitude East. Socially, it is a crossroads for all ethnic groups from diverse backgrounds. The climate is dry desert with low rainfall. On average, it rains only 40 to 80 mm/year, usually in August. Sandstorms dominate the seasons. Temperatures are very high, often reaching 45° C during hot spells (e.g. April and May), but can be severely low, reaching 5 to 15° C (November to March). There are no permanent watercourses, but the fossil water system still functions well. SOMAÏR's industrial facilities are based around 7 km from the town [9][10].

### **General study methodology**

The general methodology adopted for the study revolves around 3 points:

A preliminary phase during which contact was made with personnel from the electromechanical & refrigeration workshop, the Artois mine dewatering plant and the power station; and a literature search. A second phase of data collection and processing, consisting of an inventory of operating equipment and processing of operating data. A final phase of data analysis and interpretation.

### **The system and drainage circuit at SOMAÏR's Artois Mine**

The first method used to get rid of water at the SOMAÏR mine is to pump drainage water directly onto the surface of the mining unit. The amount of water in certain pits is becoming increasingly significant, so a permanent drainage system has become essential to manage and evacuate the various water inflows. Tanker trucks use this water to remove the dust. This system consists of one or more sumps located at the bottom of the mine, where the ore is mined, and a pumping system comprising suction and delivery pipes. If all the water inflows were combined, the sump's feed rate would constitute the pumping system's flow rate, which the mine dewatering operation would have to take into account. When there was a lot of water, eight (8) pumps were used to evacuate the water during the day and two in reserve. At present, four (4) are in use, given the low water

level, and operate 24 hours a day. These include submersible pumps, raft pumps and Godwin pumps (used on the surface). Most of the pumps used are submersible or "Hilding Flygt" submersible pumps. At SOMAÏR, secondary drainage results from water coming into the mine after blasting (using explosives) from part of the mining section (water table below the mining section) or from water located above the mining section. To recover this water, sumps or albraques are made to collect it, and submersible and raft pumps are used to pump and bring the water to a main collector. At this level, raft and surface pumps are also used to send the water from the main collector out of the mine field into a basin known as basin zero.

The dewatering circuit is nothing more than the network of pipes through which pumped water leaves a sump (albraque) or filtering well to a discharge point outside the mine field. A drainage circuit is characterized by its geometric height, fluid flow rate, suction and discharge piping, and pressure losses (singular and regular). The characteristics of the installation enable us to select the pump that will deliver the expected results (head, flow rate, etc.) under the best operating conditions. We distinguish between centrifugal pumps with impeller and diffuser, and centrifugal pumps with volute casing (Godwin). Centrifugal pumps will be used as the basis for the secondary drainage of the Artois mine.[11]

### Flygt 2201 pumps and their electrical characteristics

Code version 2201 pumps are particularly suitable for mines, quarries, road tunnels and deep excavations, as well as for serving long horizontal pipes.

Code 2201 pumps are available in two versions: aluminum or cast iron. The cast-iron model is available in three versions: MT, HT and ST, and the aluminum model in MT and HT variants. The ST pump features a vortex impeller with a Ø40 mm passage cross-section. In the event of wear, neither the impeller nor any other part of the pump needs to be adjusted.

The stator is fitted with three thermoprobes connected in series, enabling the main contactor to be controlled via an auxiliary cable (**Table 1**).

**Table 1:** Electrical characteristics of code version 2201.

|                         |      |      |      |      |      |      |      |      |      |
|-------------------------|------|------|------|------|------|------|------|------|------|
| Voltage (V)             | 190  | 200  | 220  | 380  | 400  | 415  | 440  | 500  | 550  |
| Intensities(A)          | 135  | 128  | 116  | 67   | 64   | 61   | 58   | 51   | 46   |
| Cable (mm) <sup>2</sup> | 4*50 | 4*50 | 4*35 | 4*16 | 4*16 | 4*16 | 4*16 | 4*10 | 4*10 |

**Table 2 below** shows some of the features of motor code version 2201.

**Table 2:** Motor characteristics, code version 2201 ;

| Features  | Description                         |
|---|-------------------------------------|
| Motor type                                      | Induction cage motor                |
| Frequency                                       | 50 Hz or 60 Hz                      |
| Power supply                                    | Three-phase                         |
| Start-up method                                 | Direct mode Star-delta              |
| Maximum number of starts/hour                   | 30 starts/hour at regular intervals |
| Code compliance                                 | IEC60031-1                          |
| Voltage variation supported without overheating | ±10%, if full load not permanent    |
| Tolerated voltage imbalance                     | 2%                                  |
| Stator insulation class                         | H(180°C [360°F])                    |

### Description of Godwin surface pumps

Godwin Dri-Prime pumps discharge raw effluent, sludge and liquids containing solids up to 125 mm in diameter. The pumps are self-priming up to a suction head of 8.5 m and can run dry. These pumps are available in two series: the CD series for high flow rates and medium heads, and the HL series for lower flow rates but higher heads.

The CD and HL series are available with electric or diesel engines.

The hydraulic part of these pump series is available in 316 or CD4MCu stainless steel, for pumping liquids with pH values between 2 and 12, and the motor part in cast iron or steel. With their open impeller design, Godwin Dri-Prime pumps can handle solid particles up to 125 mm in diameter.

➤ The HL series:

- Flow rate: 107 to 1200 m<sup>3</sup>/h
- Cross-sectional area: 65 mm<sup>2</sup> ;
- Head: 100 to 160 m.

### Determination of total head

The Total Head of a pump is the pressure difference in meters of water column between the suction and discharge ports.

The choice of pump depends on the characteristics of the circuit and the liquid flow rate.

To express the characteristics of a circuit numerically, we calculate its Total Manometric Head (TMH), which is given by the following formulae, depending on the assembly:

➤ Submersible or submersible pumps :

$$\text{HMT} = H_r + \sum \text{pertes} + \Delta H$$

$$H_a = 0$$

➤ Suction pumps:  $\text{HMT} = H_r + H_a + \sum \text{pertes} + \Delta H$

➤ Loaded pumps:  $\text{HMT} = H_r - H_a + \sum \text{pertes} + \Delta H$

With :

$H_a$ : suction height ;

$H_r$ : discharge head.

$$\sum \text{pertes} = \lambda \cdot \frac{l}{d} \cdot \frac{V^2}{2g} + \xi \frac{V^2}{2g} \quad (\text{m})$$

With :

$\xi$  = Pressure loss coefficient, depends on the nature and geometry of the accident". The value of  $\xi$  is given by the manufacturers in their catalogs.

$L$  = distance or length between the 2 points considered (m) ;

$d$  = pipe diameter (m) ;

$V$  = average flow velocity in the pipe (m/s);  $\rho$  = fluid density (kg/m<sup>3</sup>) ;

$g$  = acceleration of gravity (m/s<sup>2</sup>) ;

$\lambda$  = linear head loss coefficient.  $\lambda$  depends on the nature of the flow and in particular on the REYNOLDS number.

In the case of laminar flow, the coefficient  $\lambda$  obeys POISEUILLE's law:

$$\lambda = \frac{64}{Re}$$

In the case of turbulent flow and for REYNOLDS numbers between 3000 and 105 (smooth turbulent flow), the BLASIUS formula is used:

$$\lambda = 0.3164 Re^{-0.25}$$

In rough turbulent flow,  $Re > 105$ , the value of  $\lambda$  is generally read off from a chart drawn up by NIKURADSE or MOODY-MOURINE.

For industrial piping, the BLENCH formula is most often used:

$$\lambda = 0,79 \sqrt{\frac{\varepsilon}{d}}$$

$\varepsilon$  = conventional or average roughness (m) ;

$d$  = pipe diameter (m).

## Results and discussion

### Dewatering pump operating costs

#### Electricity consumption and water production

Electricity consumption (kWh) and water production (m<sup>3</sup>) for the year 2020 are shown in **Table 3**.

**Table 3:** Data on electricity consumption and water production in 2020.

| The year 2020 | Meter no. | Electricity (kWh) | Production (m) <sup>3</sup> | Specificenergy (kWh/m) <sup>3</sup> |
|---------------|-----------|-------------------|-----------------------------|-------------------------------------|
| January       | 30338     | 4957              | 2078                        | 2,39                                |
| February      | 36266     | 5928              | 6537                        | 0,91                                |
| March         | 39613     | 3347              | 5147                        | 0,65                                |
| April         | 42324     | 2711              | 4045                        | 0,67                                |
| May           | 48751     | 6427              | 5688                        | 1,13                                |
| June          | 55434     | 6683              | 4561                        | 1,47                                |
| July          | 61408     | 5974              | 4561                        | 1,31                                |
| August        | 67632     | 6224              | 4744                        | 1,31                                |
| September     | 81878     | 14246             | 9344                        | 1,52                                |
| October       | 94334     | 12456             | 10184                       | 1,22                                |
| November      | 95295     | 961               | 616                         | 1,56                                |
| December      | 118617    | 23322             | 19731                       | 1,18                                |
| <b>Total</b>  |           | <b>93236</b>      | <b>77236</b>                | <b>15,32</b>                        |

Note that specific energy is defined as the ratio of electricity consumption to monthly water production.

The data in **Table 4** are the readings for electricity consumption and water production for the year 2021. Empty cells indicate that there was no dewatering either (May and April).

**Table 4:** Data on electricity consumption and water production in 2021.

| The year 2021 | Meter no. | Electricity (kWh) | Production(m) <sup>3</sup> | Specificenergy (kWh/m) <sup>3</sup> |
|---------------|-----------|-------------------|----------------------------|-------------------------------------|
| January       | 128162    | 9545              | 8598                       | 1,11                                |
| February      | 145854    | 17692             | 13623                      | 1,30                                |
| March         | 155161    | 9307              | 6978                       | 1,33                                |
| April         | 155249    | 88                |                            |                                     |
| May           | 155288    | 39                |                            |                                     |

|              |        |               |               |      |
|--------------|--------|---------------|---------------|------|
| June         | 182973 | 27685         | 23630         | 1,17 |
| July         | 193600 | 10627         | 8327          | 1,28 |
| August       | 197796 | 4196          | 946           | 4,44 |
| September    | 205870 | 8074          | 5808          | 1,39 |
| October      | 226952 | 21082         | 17602         | 1,20 |
| November     | 241103 | 14151         | 12218         | 1,16 |
| December     | 255087 | 13984         | 12318         | 1,14 |
| <b>Total</b> |        | <b>136470</b> | <b>110033</b> |      |

**Table 5 shows** electricity consumption and water production in (m<sup>3</sup>) for the year 2022.

*Table 5: Data on electricity consumption and water production 2022.*

| The year 2022 | Meter no. | Electricity (kWh) | Production(m ) <sup>3</sup> | Specificenergy (kWh/m ) <sup>3</sup> |
|---------------|-----------|-------------------|-----------------------------|--------------------------------------|
| January       | 265507    | 10420             | 9311                        | 1,12                                 |
| February      | 279607    | 14100             | 10823                       | 1,30                                 |
| March         | 291665    | 12058             | 10525                       | 1,15                                 |
| April         | 305419    | 13754             | 11370                       | 1,21                                 |
| May           | 321139    | 15720             | 10795                       | 1,46                                 |
| June          | 338841    | 17702             | 13732                       | 1,29                                 |
| July          | 348964    | 10123             | 8426                        | 1,20                                 |
| August        | 367651    | 18687             | 14211                       | 1,31                                 |
| September     |           |                   |                             |                                      |
| October       |           |                   |                             |                                      |
| November      |           |                   |                             |                                      |
| December      |           |                   |                             |                                      |
| <b>Total</b>  |           | <b>112564</b>     | <b>89193</b>                |                                      |

### Summary of energycosts

The average price per kWh billed to SOMAÏR over the three (3) years is **170F** for the months of March to November and **190F** for the months of January-February-December.

- For the year 2020: the total energy consumption is **93,236 kWh** and the total volume of water pumped **77,236 m<sup>3</sup>** at a cost of **16,534,260 FCFA**.
- For the year 2021: total energy consumption is **136,470 kWh** and the volume of water pumped **110,033 m<sup>3</sup>** at a cost of **24,024,320 FCFA**.
- For the year 2022: total energy consumption is **112,564 kWh** and the volume of water pumped **89,193 m<sup>3</sup>**, at a cost of **19,626,280 FCFA**.

For the three (3) years, the total cost is **60,184,860 FCFA**.

It should be noted that when the Société Nigérienne du Charbon (SONICHAR) line is not available, SOMAÏR starts up its back-up line (generators), each of which consumes **400 liters of diesel** per hour. The average consumption of a set is estimated at **0.29 liters/kWh**, and one (1) liter of diesel costs **450F**.

In order to optimize and monitor the operation of the Artois pit drainage facilities, three (3) annual specific energy ratios have been studied.

The graph in **Figure 2**, based on the data in **Table 3**, shows the monthly variation in water production for the year 2020. The variation in specific energy corresponding to the electrical energy consumed to produce one (1) m<sup>3</sup> of water is also shown. The variation in ratios enables us to assess the performance of the drainage system's equipment. Outside the months of February, March and April, water production is lower than electricity consumption (**figure 2**), **resulting** in excess electricity consumption.

The monthly operating amplitudes of SOMAÏR's Artois mine dewatering system in 2020 are as follows:

- Production peaks in December with 19,731 m<sup>3</sup> /month;
- SONICHAR/backup generator consumption reached 23,322 kWh, corresponding to a specific consumption of 1.18 kWh/m<sup>3</sup> ;
- The year's production trough was reached in November with 616 m<sup>3</sup> corresponding to a specific consumption of 1.56 kWh/m<sup>3</sup> .

It should be noted that the energy supplied by emergency generators has been taken into account in the electricity consumption figures. The average specific consumption in 2020 is 1.27 kWh/m<sup>3</sup>.

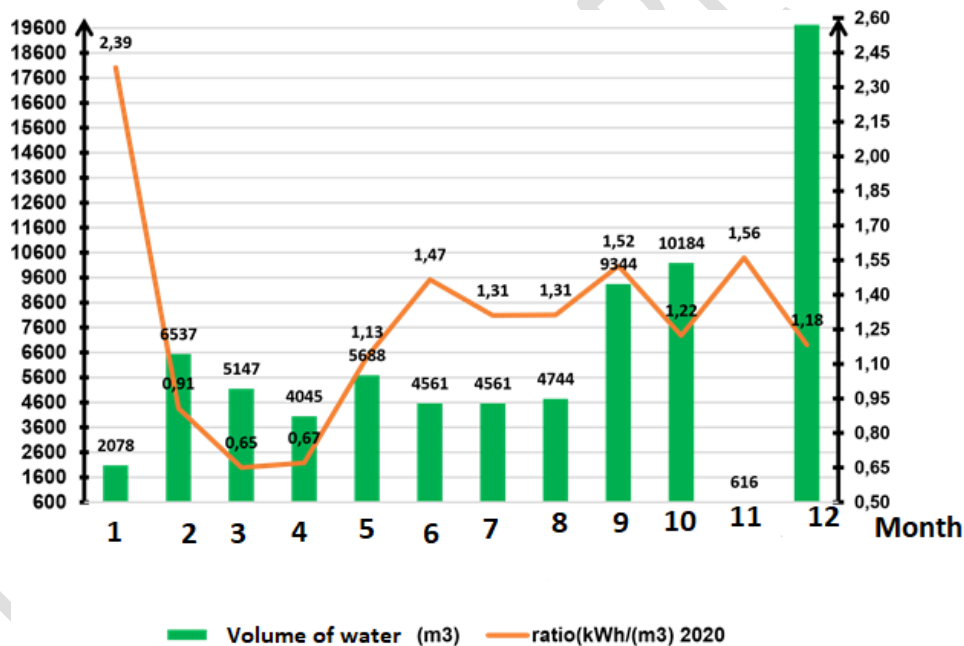


Figure 2: Illustration of water volume (m<sup>3</sup>) and ratio for the year 2020.

The graph in **Figure 3**, drawn from the data in **Table 4**, shows the monthly variation in water production and the corresponding ratios for the year 2021.

For the year 2021, with the exception of April and May when there was no dewatering, for all other months the volume of water pumped out of the mine field is less than the electricity consumption, corresponding to overconsumption.

In a good pumping system, the volume of water pumped must be greater than the energy consumed if we are to speak of the effectiveness and efficiency of the pumps installed.

Pumps used to drain water are characterized by excessive consumption.

The monthly operating amplitudes of SOMAIR's Artois mine dewatering system in 2021 are as follows:

- Production peaks in December with 23,630 m<sup>3</sup> /month;
- SONICHAR/standby generator consumption reached 27,685 kWh, corresponding to a specific consumption of 1.17 kWh/m<sup>3</sup> ;
- The year's production trough corresponds to the months of April and May when there is no dewatering.

Here too, the energy supplied by emergency generators has been taken into account in the electricity consumption figures. The average specific consumption in 2021 is 1.55 kWh/m<sup>3</sup>.

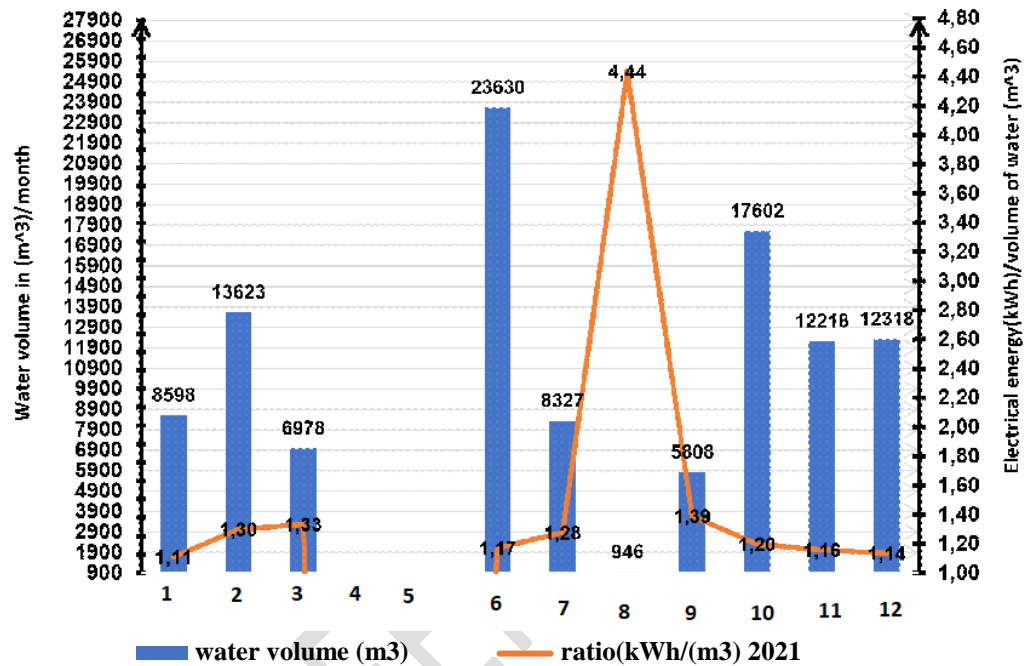


Figure 3: Illustration of water volume (m<sup>3</sup>) and ratio for the year 2021.

The graph in figure 4 shows the monthly variation in water production for the year 2022 and the corresponding ratios.

In 2022, the specific energy shows that consumption is greater than the volume of water (m<sup>3</sup>) drained from the mine field. This means that the pumps are oversized.

The monthly operating amplitudes of SOMAIR's Artois mine dewatering system in 2022 are as follows:

- Production peaks in August with 14,211 m<sup>3</sup> /month;
- SONICHAR/backup generator consumption reached 18,687 kWh for a specific consumption of 1.31 kWh/m<sup>3</sup> ;
- Production peaked in July, with 8,426 m<sup>3</sup> /month for a specific consumption of 1.29 kWh/m<sup>3</sup> .

As in the first two cases, the energy supplied by emergency generators was also included in the year's electricity consumption.

2022.

Average specific consumption in 2022 is 1.25 kWh/m<sup>3</sup>.

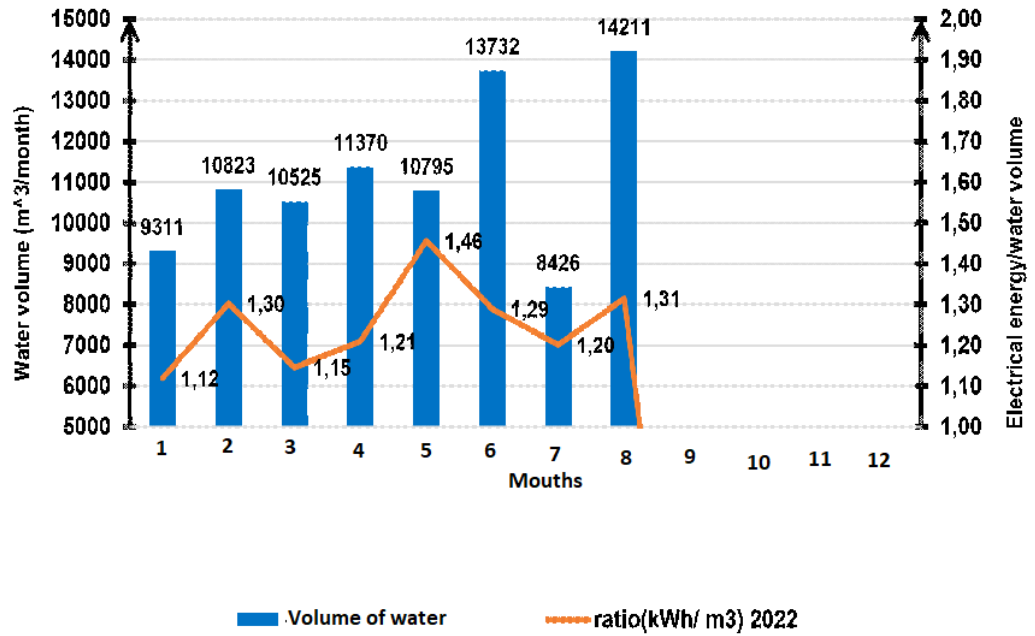


*Figure 4: Illustration of volume (m<sup>3</sup>) and ratio for the year 2022.*

Ratios for 2020, 2021 and 2022 by month are shown in **Figure 5**.

The peaks appear (**Figure 5**) in August for the year 2021, followed by January 2020 and May 2022.

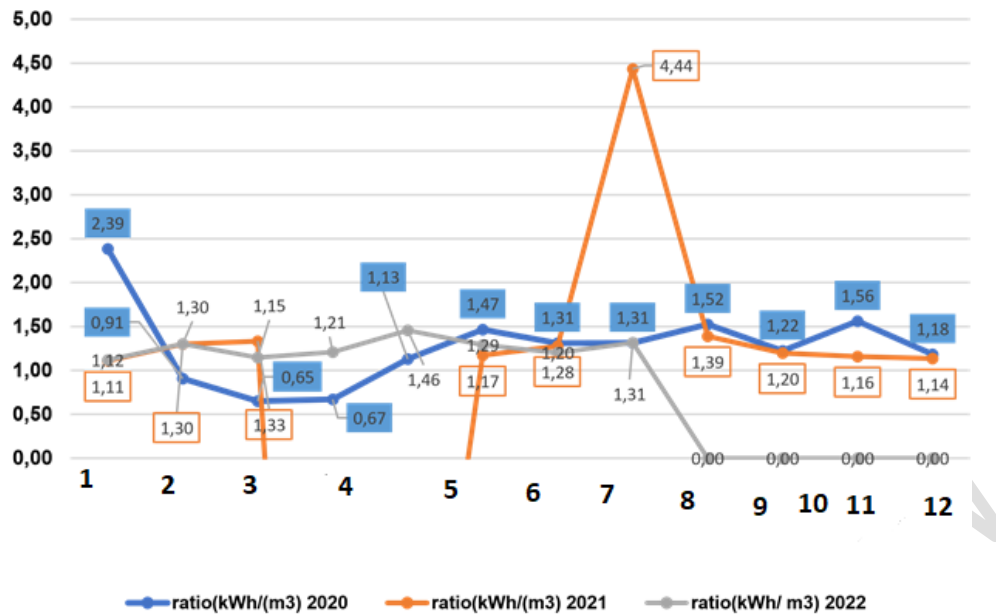


Figure 5: Comparison of ratios for the three years.

The disc chart in figure 6 shows high electricity consumption for the year 2021, followed by 2022 and then 2020.

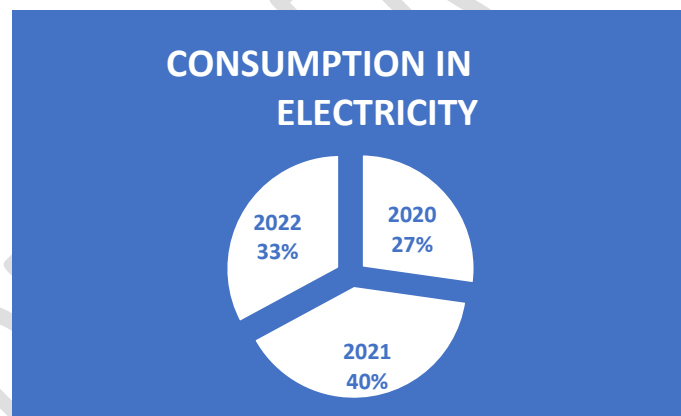


Figure 6: Illustration of electricity consumption over the three years.

The characteristics recorded on the nameplates of the pumps (FLYGT and Godwin) used to extract the water drained from the SOMAIR mine floor are given in Table 4. Figure 7: Illustration of excess water over the three years.

**Table 6:** Nameplates for Flygt and Godwin pumps.

|   |              |                 |          |                              |                |
|---|--------------|-----------------|----------|------------------------------|----------------|
| Flygt 2201,012-177035: HP pump (high pressure) weight 240 kg              |              |                 |          |                              |                |
| Three-phase motor: TP 111CL.HIEC60034-1                                   |              |                 |          |                              |                |
| Power   | Voltage      | Intensity       | Coupling | Power factor                 | Rotation speed |
| 37 kW   | 690/400 V    | 37/65A          | Y/Δ      | CosΦ = 0.92                  | 2940 rpm       |
| Pump output flow  |              |                 |          | 80 to 83 m <sup>3</sup> /h   |                |
| Maximum temperature :   |              |                 |          | 40 °C                        |                |
| Length to discharge hose :  |              |                 |          | 120 m                        |                |
| Godwin: surface pump  |              |                 |          |                              |                |
| Type: AU-DF280S-HIE2 ; series : 280A942403 ; 50Hz ; 60Hz ; weight :530 Kg |              |                 |          |                              |                |
| Power   | Voltage (V)  | Current (A)     | Coupling | Speed                        |                |
| • 75 kW   | 400 Δ/690 Y  | 132/76.7 (50Hz) | • Y/Δ    | 1480 rpm                     |                |
| • 90 kW   | 480 Δ /830 Y | 132/76.7 (60Hz) | • Y/Δ    | 1775t r/min                  |                |
| Conveyed flow   |              |                 |          | 102 to 104 m <sup>3</sup> /h |                |

All pumping applications have three things in common:

- ❖ The flow rate, which is the quantity of liquid pumped per unit of time;
- ❖ The total geometric height, which represents the height between the point of extraction and the discharge ;
- ❖ Singular load losses caused by narrowings, widenings and other accidents (elbows, tees, etc.);
- ❖ Regular head losses, due to friction as the fluid moves through the pipes.

FLYGT version code 2201,012 high-pressure (HP) pump: performance verification.

Consider the characteristics of the high-pressure (HP) pump code version 2201,012:

- Flow rate at pump discharge port:  $Q = 83 \text{ m}^3 / \text{h} = 23.05 \text{ l/s}$  ;
- Power  $P = 37 \text{ kW}$  ;
- Industrial water:  $\rho = 1100 \text{ kg/m}^3$  ;
- Dischargelength  $L_r = 120 \text{ m}$  ;
- Head  $H_g = 10 \text{ m}$
- Dischargediameter:  $\varnothing 80 \text{ mm}$ .

$$\text{HMT} = H_g + \sum p_{ertes} + \Delta H \quad \text{with suction height } H_a = 0 \text{ m (submersible pump)}$$

$$\Delta H = 0 \text{ m.}$$

Considering singular pressure losses equal to 20% of the discharge head, and linear pressure losses equal to 10% of the discharge length [9].

$$\text{HMT} = 10 + 2 + 12 = 24 \text{ m}$$

$$P_{\text{hyd}} = \rho \cdot g \cdot Q_v \cdot \text{HMT} = \frac{1100 \times 9.81 \times 83 \times 24}{3600} = 5.97 \text{ kW}$$

$$\eta = \frac{P_{hyd}}{P_{abs}} = \frac{5,97}{37} = 16,13\%$$

The above calculations show a mediocre yield.

Let's find out what flow rate corresponds to a good efficiency for a HMT equal to 24 m, since it's the HMT that is decisive in verifying a pump's performance.

For this 24 m height, flow rates and yields are as follows (**Figure 7**):

- MT 261 medium-pressure pump:  $Q = 49 \text{ l/s}$  or  $176.4 \text{ m}^3/\text{h}$ ;  $\eta = 34.3\%$ .
- HT 259 high-pressure pump:  $Q = 59 \text{ l/s}$  at  $212.4 \text{ m}^3/\text{h}$ ;  $\eta = 41.3\%$ .
- LT 234 low-pressure pump:  $Q = 105 \text{ l/s}$  or  $378 \text{ m}^3/\text{h}$ ;  $\eta = 73.5\%$ .

The pump operates at best efficiency (73.5%). Corresponding to a flow rate of 105 l/s is obtained with the low-pressure pump.

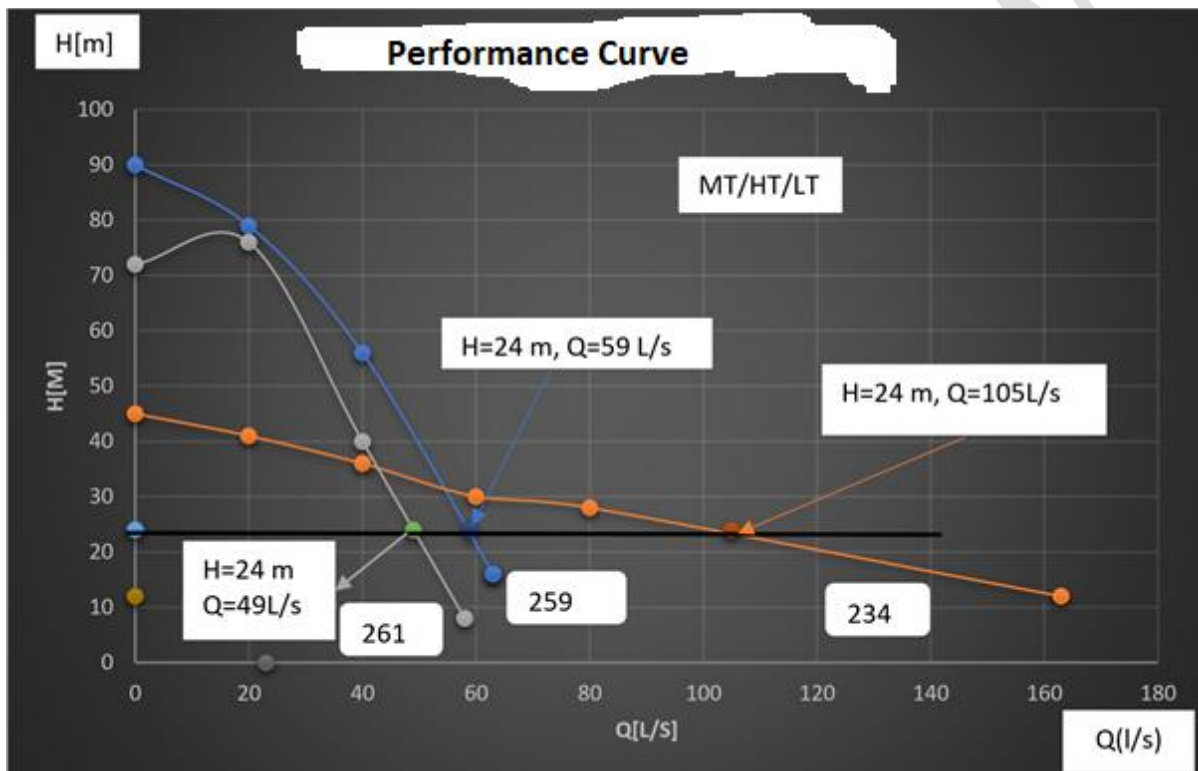


**Figure8:** Performance curves  $H = f(Q)$ .

According to the graph of performance curves  $P = f(Q)$  (**figure 2**), the powers obtained for the flows corresponding to the 24 m height are as follows:

- Pump 261:  $P = 25 \text{ kW}$  at flow  $Q = 49 \text{ l/s}$  ;
- Pump 259:  $P = 35 \text{ kW}$ , flow  $Q = 59 \text{ l/s}$  ;
- Pump 234:  $P = 35 \text{ kW}$  at flow  $Q = 105 \text{ l/s}$ .

These observations show that even the 234 low-pressure pump can ensure correct operation of the hydraulic circuit.

## Conclusion

These studies show that the design of an optimized dewatering system must take into account the nature of the fluid to be pumped, the flow rate and the total head. The energy balance for the three (3) years of pumping was drawn up using the electricity consumption data received. Peaks appear in August for 2021, followed by January 2020 and May 2022. The results show that specific energy is

high, resulting in higher power consumption than water production. According to the graph of performance curves  $P = f(Q)$ , the powers obtained for flows corresponding to the 24 m height are 25 kW at a flow rate  $Q = 49$  l/s for pump 261; 35 kW, at a flow rate  $Q = 59$  l/s for pump 259 and 35 kW at a flow rate  $Q = 105$  l/s for pump 234. These observations show that even the low-pressure pump 234 can ensure correct operation of the hydraulic circuit. This led us to take the flow rates of pumps currently in service, where we have The plotting of performance curves showed that the installed pumps are not operating at peak efficiency. Recommendations have been made to this effect.

## References

- [1] Rózkowski, K., Zdechlik, R., & Chudzik, W. (2021). *Open-pit mine dewatering based on water recirculation-Case study with numerical modelling*. *Energies*, 14(15), 4576.
- [2] Hu, L., Zhang, M., Yang, Z., Fan, Y., Li, J., Wang, H., & Lubale, C. (2020) *Estimating dewatering in an underground mine by using a 3D finite element model*. *Plos one*, 15(10), e0239682.
- [3] El Idrysy, H.; Connelly, R. *Water-the Other Resource a Mine Needs to Estimate*. *Procedia Eng*. 2012, 46, 206-212.
- [4] Sahoo, L. K., Bandyopadhyay, S., & Banerjee, R. (2014). *Water and energy assessment for dewatering in opencast mines*. *Journal of cleaner production*, 84, 736-745.
- [5] Michlowicz, E., & Wojciechowski, J. (2021). *Energy consumption analysis of the main dewatering pumps in underground mines*. *Mining-Informatics, Automation and Electrical Engineering*, 59(2).
- [6] Van der Wateren, W., Joubert, H. P. R., & Kleingeld, M. (2018, August). *Optimising energy recovery in mine dewatering systems*. In *2018 International Conference on the Industrial and Commercial Use of Energy (ICUE)* (pp. 1-8). IEEE.
- [7] Du Plessis, E. P. J. (2020). *Investigating the dewatering energy savings potential of an open pit mine (Doctoral dissertation, North-West University (South Africa))*.
- [8] Smith, T., Joubert, H. P. R., & Van Rensburg, J. F. (2015, August). *Automated control of mine dewatering pumps to reduce electricity cost*. In *2015 International Conference on the Industrial and Commercial Use of Energy (ICUE)* (pp. 62-69). IEEE.
- [9] A. Tadewal, B.D. Farida, K. Moussa and B. Ousmane "Hydrogeological characterization of the Izegouande Permian aquifer (Tim Mersoï Basin, North Niger) " *American Journal of Sciences and Engineering Research*, 4 (5) 2021 12-23
- [10] Daou, I. E., Harouna, S., Hassan, A. M., Charzynski, P., Switoniak, M., & Badjo, A. T. D. (2022). *Assisted Radiological Stabilization and Monitoring of Radon Fluxes and Gamma Irradiations of Residues from the Processing of Uranium Ore of Arlit Mines (Northern Niger) Using Multivariate Statistical Methods and the Geotechnical Approach*. *Journal of Materials and Environmental Science*. Volume 13, Issue 12, Page 1354-1369
- [11] M.IDRISSA HAMADOU Marou, *Coût d'exploitation de l'électropompe dans l'exhaure mine, Département electromecanique, Ecole des Mines de l'industrie et de la Géologie, Mémoire de fin de cycle Ingénieur, 2020, 70 pages*